Synthesization of ZnO nanomaterials

Jong-Soo Lee, Byung-Don Min, and Sang-Sig Kim*
Department of Electrical Engineering, College of Engineering, Korea University, Anam-dong, Seongbuk-gu, Seoul 136-701, Korea

*E-mail: sangsig@korea.ac.kr

(Received 16 April 2003, Accepted 19 May 2003)

ZnO nanobelts, nanorods, and nanowires were synthesized at three different substrate temperatures from the thermal evaporation of ball-milled ZnO powders at 1380 ℃. Transmission electron microscopy (TEM) revealed that the ZnO nanobelts are single crystalline with the growth direction perpendicular to the (010) lattice planes, and that the ZnO nanorods and nanowires are single crystalline with the growth directions perpendicular to the (001) and (110) lattice planes, respectively. In cathodoluminescence (CL), the peak energy of near band-edge (NBE) emission was determined for nanobelts, nanorods, and nanowires.

Keywords : ZnO nanowire, Nanobelt, Nanorod, Ball-milling, Cathodoluminescence

1. INTRODUCTION

Direct-gap ZnO semiconducting material (E_g = 3.37 eV at 25 °C) is one of the attractive candidates for high efficient optical devices operating at room temperature, since excitons formed in this material have a high binding energy of 60 meV[1,2], compared with other semiconducting materials (for instance, exciton binding energy is 22 meV for ZnSe, and 25 meV for GaN)[3,4]. Such a high exciton binding energy disables a role of phonons at room temperature since this binding energy is larger by 2.4 times than the effective thermal energy. Because of this reason, ZnO material emits efficient exciton emissions at high temperatures up to 550 K under low excitation energy[5].

The synthesis of nanostructured semiconducting materials has become one of important research issues since a notable discovery of graphitic nanotubes[6]. Compound semiconducting nanomaterials including GaN[7,8], GaP[9], InP[10], ZnO[11,12], and Ga_2O_3[13] have been developed for the fabrication of nano-optoelectronic devices. In particular, the nanomaterials of metal-oxide-related semiconductors such as ZnO and Ga_2O_3 have been a matter of concern due to their excellent crystalline quality, chemical stability, thermal stability, and wide bandgap. Ga_2O_3 nanobelts were synthesized previously by the thermal evaporation of GaN powders in our group, and their structural and optical properties have been reported in Refs.14 and 15. In this study, the synthesis of ZnO nanomaterials by thermal evaporation of ball-milled ZnO powders and their structural and optical characteristics were investigated.

This paper presents the structural and optical properties of three different nanostructured ZnO materials (nanowires, nanobelts, and nanorods) synthesized from thermal evaporation of ball-milled ZnO powders. A comparison of these three nanomaterials is first made by scanning electron microscopy (SEM) and transmission electron microscopy (TEM), and their optical properties are then characterized by cathodoluminescence (CL).

2. EXPERIMENTAL

ZnO powders (-200 mesh) were used for synthesizing nanomaterials under study. The ZnO powders were first ground for 20 hours in the mechanical ball mill system using a steel vial with 100 stainless steel balls, in which the mixture ratio of steal balls and ZnO powders was 15:1 in weight percents. An alumina boat containing the ball-milled ZnO powders was then loaded into the center of a horizontal alumina tube and 5×5 mm sized Si substrates were put at three different places in the tube (Fig. 1). The thermal evaporation of the ball-milled ZnO powders was performed at 1380 ℃ for 3 hours with an argon flow rate of 500 standard cubic centimeters per minute (sccm) under a constant furnace chamber pressure of 0.5 atm.

The as-synthesized products were characterized by X-ray diffractometer diffraction (RIGAKU, D/MAX-⌐A), field emission scanning electron microscope (HITACHI, S-4700), and transmission electron microscopy (JEOL, JEM 3000F) for the analysis of the microstructure. Room-temperature CL(monoCL2, Gatan) was performed at an acceleration voltage of 5kV.

3. RESULTS AND DISCUSSION

Figure 1 shows the scanning electron microscopy images of nanomaterials synthesized in three different zones in the furnace tube; the temperature ranges of the three zones labeled A, B, and C are 1030~900, 700~650, and 450~350 ℃, respectively. A comparison of the three SEM images illustrates that morphologies of three nanomaterials synthesized at different substrate temperatures are distinctively different each other.

The SEM image of Fig. 1(a) exhibits that nanomaterials synthesized in the A zone are mixtures of nanobelts and nanorods; nanomaterials having their rectangular cross section are named nanobelts, and nanomaterials having their hexagonal cross section are named nanorods (see the insert of Fig. 1(b). The nanobelts and nanorods synthesized in the A (1030~900 ℃) zone are in the range of several hundred nanometers to several hundred micrometers in width or in diameter. The SEM image of Fig. 1(b) reveals that nanomaterials synthesized in the B (700~650 ℃) zone are also mixtures of nanobelts and nanorods, but that their sizes are in the range of 70 to 300 nm. In contrast, the SEM image of Fig. 1(c) shows that nanomaterials synthesized in the C (450~350 ℃) zone are nanowires; nanomaterials having their circular cross section are named nanowires (see the insert of Fig. 1(c)). The nanowires are in the range of 15 to 40 nm in diameter and in the range of 10 to 70 μm in length; their diameter and length are very uniform, compared with the nanobelts and nanorods.

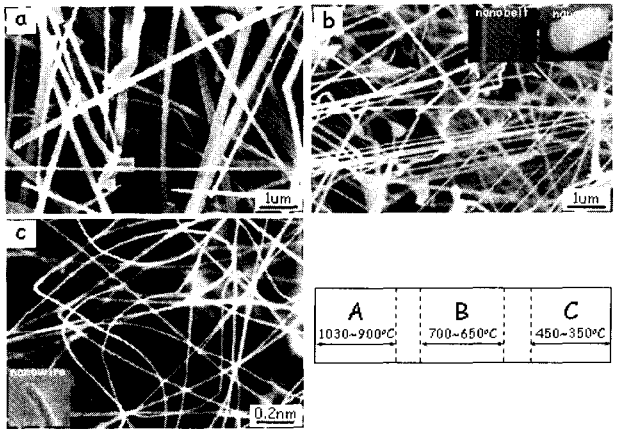

Fig. 1. SEM images of the ZnO nanomaterials grown in (a) A zone (1030~900℃), (b) B zone (700~650℃), and (c) C zone (450~350℃).

Figure 2 shows the X-ray diffraction (XRD) patterns of starting ZnO powders, ball-milled ZnO powders, and as-synthesized ZnO nonomaterials. The XRD pattern of the starting ZnO powders (Fig. 2(a)) is indexed to the wurtzite hexagonal structure. For the ball-milled ZnO powders, the XRD peaks are diminished in intensity and broadened in line width (Fig. 2(b)). The representative XRD pattern of three as-synthesized ZnO materials (Fig. 2(c)) is identical to that of the starting ZnO powders, so the nanomaterial products are identified to be ZnO; XRD patterns of all the nanomaterials synthesized in the A, B, and C zones are the same.

The SEM image in Fig. 3 exhibits the side view of the nanomaterials grown on a Si substrate in the B zone. This image shows that the nanobelts and nanorods are grown not from the Si substrate but from a thick layer of ZnO polycrystalline material on the top of the Si substrate, indicating that the thick layer is formed before the formation of the nanowires. This observation implies that the XRD pattern of the materials grown on a Si substrate in the B zone (Fig. 1(b)) comes not only from the nanomaterials but also from the thick layer. The SEM images of the materials grown on Si substrates in the A and C zones show also the presence of the thick layers of ZnO polycrystalline material on the top of Si substrates.

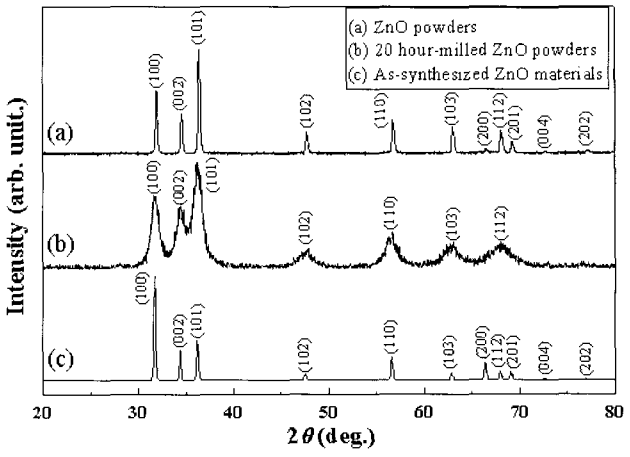

Fig. 2. The XRD patterns of (a) starting ZnO powders, (b) ball-milled ZnO powders, and (c) synthesized ZnO materials.

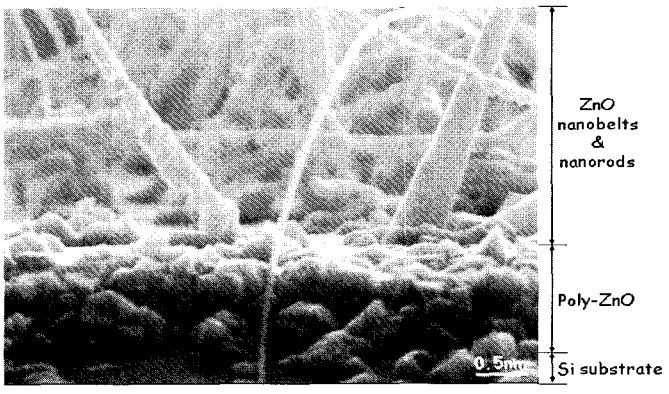

Fig. 3. The side view image of the materials grown on a Si substrate in the B zone.

Both the nanomaterials (nanobelts, nanorods, and nanowires) and the thick layer may be ZnO materials, since any other peaks but the peaks related to the ZnO hexagonal phase are not seen in the XRD patterns. Nevertheless, a possibility that the nanobelts, nanorods, and nanowires are not ZnO material is still not ruled out on this stage.

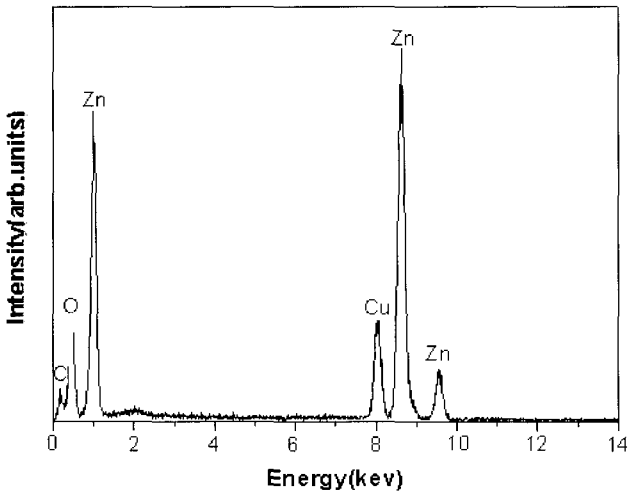

Fig. 4. The energy dispersive X-ray (EDX) spectrum of the nanomaterials.

A representative energy dispersive X-ray (EDX) spectrum of the nanomaterials (nanobelts, nanorods, and nanowires) is depicted in Fig. 4. Only the peaks associated with Zn and O atoms are seen in this EDX spectrum (the Cu-related peak in the spectrum comes from the Cu grids), leading to the obvious fact that the nanobelts, nanorods, and nanowires are indeed ZnO material.

Figure 5 shows transmission electron microscopy (TEM) images of three selected nanomaterials(a nanobelt nanorod are selected from the nanomaterials synthesized in the B zone, and the nanowire is selected from the to the nanomaterials synthesized in the C zone. The insets of Figs. 5(a), 5(b) and 5(c) show three representative selected-area electron diffraction (SAED) patterns taken from these nanomaterials. In the SAED patterns, the direction of the zone axe is indexed to be the [100] lattice direction for the nanobelt (Fig. 5(a)), the [100] lattice direction for the nanorod (Fig. 5(b)), and the [100] lattice direction for the nanowire (Fig. 5(c)). The SAED reveals that the direction of the growth is perpendicular to the (010) lattice planes for the nanobelt (Fig. 5(a)), to the (001) lattice planes for the nanorod (Fig.(a), a nanorod (b), and a nanowire (c)); the nanobelt and 5(b)), and to the (110) lattice planes for the nanowire (Fig. 5(c)). On the basis of the TEM, SAED, and SEM analyses, the orientations of hexagonal lattice units in the nanobelts, nanorods, and nanowires may be determined.

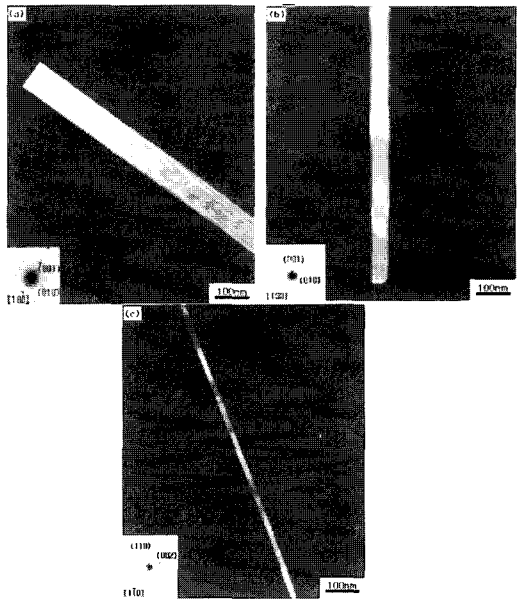

Fig. 5. The TEM bright field images and their associated SAED patterns of a selected nanobelt(a), a selected nanorod (b), and a selected nanowire(c).

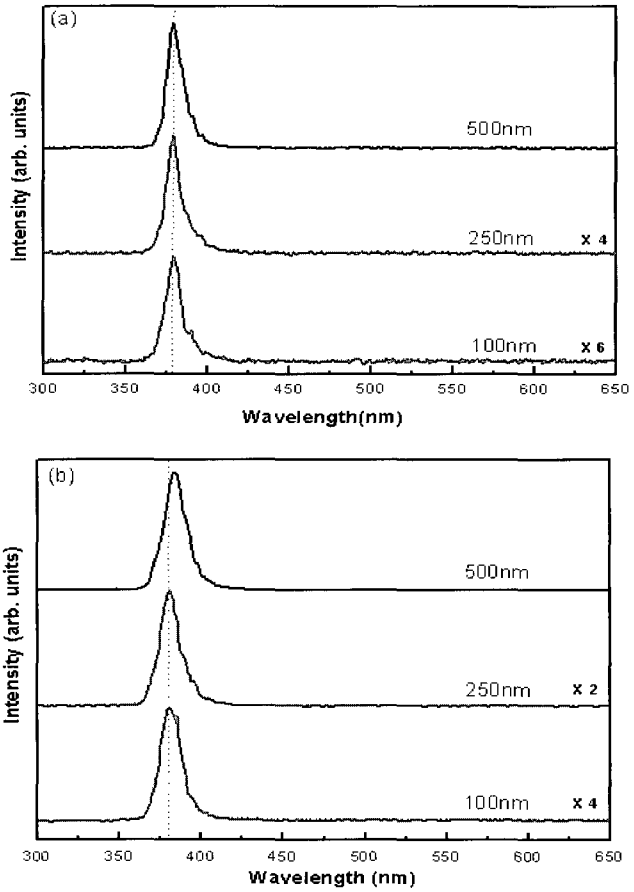

Fig. 6. The room temperature(300K) CL spectra of the ZnO nanobelts(a) and nanorods(b) selected from the nanomaterials synthesized in the B zone.

Figure 6 exhibits size-selective CL spectra for six single nanobelts and nanorods selected from the nanomaterials synthesized in the B zone. The energy position of the near band-edge (NBE) peak is the same (3.280 eV) for the 100-, 250-, and 500-nm thick nanobelts. For the nanorod, the energy position of the NBE peak is the same (3.262 eV) for the 100 -and 250-nm thicknesses, but the energy position of the 500-nm thickness is 3.237 eV. Note that the NBE emission peaks are responsible for the recombination of free excitons. As the energy position of the NBE peak follows the bandgap, the bandgap of the nanobelts is independent of their size in the size range of 100 nm to 500 nm, but the bandgap of the nanorod is not independent. In this size range, the band gap depends not on the quantum confinement but on strain experienced entirely by nanomaterials[16]. Thus, the 500-nm thick nanorod may be experienced by tensile strain, compared with the other 100- and 250-nm thick nanorods.

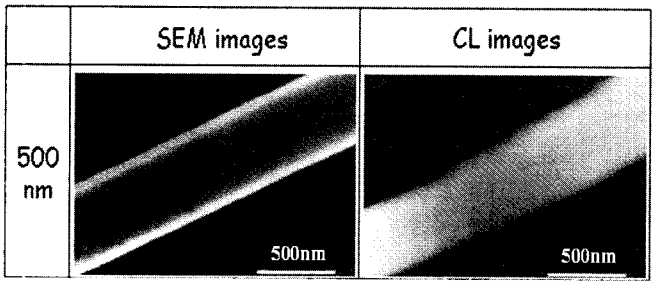

Fig. 7. The SEM image and CL image of 500-nm thick ZnO nanobelt selected from the nanomaterials synthesized in the B zone.

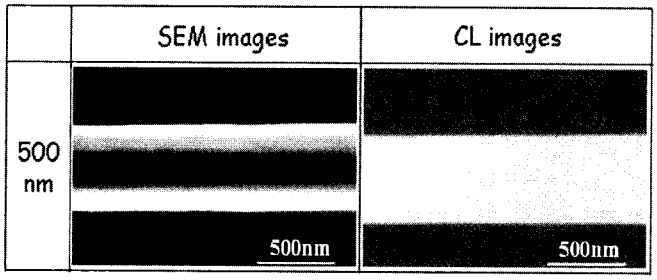

Fig. 8. The SEM image and CL image of 500-nm thick ZnO nanorod selected from the nanomaterials synthesized in the B zone.

The size-selective SEM and CL images of the nanobelts and nanorods were shown in Figs. 7 and 8, respectively. The CL images each were detected at the NBE peak positions of the corresponding CL spectra shown in Fig. 7. The CL images reveal that the whole regions of the nanobelts and nanorods emit homogeneously the NBE emission; they do not show any dead spots that can not emit the NBE emission.

4. CONCLUSION

ZnO nanobelts, nanorods, and nanowires were synthesized at three different substrate temperatures from the thermal evaporation of ball-milled ZnO powders at 1380℃. SEM revealed that the nanobelts and nanorods synthesized in the substrate temperature (1030~900 ℃) zone are in the range of several hundred nanometers to several hundred micrometers in width or in diameter, that nanobelts and nanorods synthesized in the substrate temperature (700~650 ℃) zone are in the range of 70 to 300 nm in width or in diameter, and that the nanowires synthesized in the substrate temperature (450~350 ℃) zone are in the range of 15 to 40 nm in diameter. TEM revealed that the ZnO nanobelts, nanorods, and nanowires are single crystalline with the growth direction perpendicular to the (010), (001) and (110) lattice planes, respectively. In addition, the energy position of the near band-edge (NBE) peak is 3.280 eV for the 100-, 250-, and 500-nm thick nanobelts, 3.262 eV for the 100- and 250-nm thick nanorods, and 3.237 eV for the 500-nm thick nanorods. The CL images reveal that the whole regions of the the nanobelts and nanorods emit homogeneously the NBE emission.

ACKNOWLEDGEMENTS

This work was supported by the Korean Ministry of Science and Technology as a part of the '02 Nuclear R&D Program, Grant No. 1999-2-302-017-5 from the Basic Research Program of the Korea Science & Engineering Foundation, the '02 Hanbit Project of the Korea Basic Science Institute, and the MOST(the National Research Lavoratory Program).

REFERENCES

[1] J. M. Hvam, "Temperature-induced wavelength shift of electron-beam-pumped laser from CdSe, CdS, and ZnO", Phys. Rev., Vol. B4, No. 12, p. 4459, 1971.

[2] R. F. Service, "Will UV lasers beat the blues?", Science, Vol. 276, No. 5314, p. 895, 1997.

[3] M. H. Huang, S. Mao, H. Feick, H. Yan, Y. Wu, H. Kind, E. Weber, R. Russo, and P. Yang, "Room-temperature ultraviolet nanowire nanolasers", Science, Vol. 292, No. 5523, p. 1897, 2001.

[4] Y. F. Chen, D. M. Bagnall, H. Koh, K. Park, K. Hiraga, Z. Zhu, and T. Yao, "Plasma assisted molecular beam epitaxy of ZnO on c-plane sapphire: growth and characterization", J. Appl. Phys., Vol. 84, No. 7, p. 3912, 1998.

[5] D. M. bagnall, Y. F. Chen, Z. Zhu, T. Yao, M. Y. Shen, and T. Goto, "High temperature excitonic stimulated emission from ZnO epitaxial layers", Appl. Phys. Lett., Vol. 73, No. 8, p. 1038, 1998.
[6] N. Hamada, S. Sawada, and A. Oshiyama, "New one-dimensional conductors:graphitic microtubles", Phys. Rev. Lett., Vol. 68, No. 10, p. 1579, 1992.
[7] W. Han, S. Fan, Q. Li, and Y. Hu, "Synthesis of gallium nitride nanorods through a carbon nanotube-confined reaction", Science, Vol. 277, No. 5330, p. 1287, 1997.
[8] J. Y. Li, X. L. Chen, Z. Y. Qiao, Y. G. Cao, and Y. C. Lan, "Formation of GaN nanorods by a sublimination method", J. Cryst. Growth, Vol. 213, No. 3-4, p. 408, 2000.
[9] W. S. Shi, Y. F. Zheng, N. Wang, C. S. Lee, and S. T. Lee, "Microstructures of gallium nitride nanowires synthesized by oxide-assisted method", Chem. Phys. Lett., Vol. 345, No. 5-6, p. 377, 2001.
[10] X. Duan, Y. Huang, Y. Cui, J. Wang, and C. M. Lieber, "Indium phosphide nanowires as building blocks for nanoscale electronic and optoelectronic devices", Nature, Vol. 409, No. 6816, p. 66, 2001.
[11] Z. W. Pan, Z. R. Dai, and Z. L. Wang, "Nanobelts of semiconducting oxides", Science, Vol. 291, No. 5510, p. 1947, 2001.
[12] M. H. Huang, Y. Wu, H. Feick, N. Tran, E. Weber, and P. Yang, "Catalytic growth of zinc oxide nanowires by vapor transport", Adv. Mater., Vol. 13, No. 2, p. 113, 2001.
[13] H. Z. Zhang, Y. C. Kong, Y. Z. Wang, X. Du, Z. G. Bai, J. J. Wang, D. P. Yu, Y. Ding, Q. L. Hang, and S. Q. Feng, "Ga_2O_3 nanowires prepared by physical evaporation", Solid State Communication, Vol. 109, No. 11, p. 677, 1999.
[14] B. C. Kim, K. T. Sun, K. S. Park, K. J. Im, T. Noh, M. Y. Sung, S. Nahm, Y. N. Choi, S. S. Park, and S. Kim, "β-Ga_2O_3 nanowires synthesized from milled GaN powders", Appl. Phys. Lett., Vol. 80, No. 3, p. 479, 2002.
[15] J.-S. Lee, K. Park, S. Nahm, S. Kim, and S. Kim, "Ga_2O_3 nanomaterials synthesized from ball-milled GaN powders", J. Crys. Growth, Vol. 244, No. 3-4, p. 287, 2002.
[16] K. Park, J. –S. Lee, M. –Y. Sung, and S. Kim, "Structural and optical properties of ZnO nanowires synthesized from ball-milled ZnO powders", Jpn. J. Appl. Phys., Vol. 41, p. 7317, 2002.